JOURNAL OF SOLID STATE CHEMISTRY 58, 103–113 (1985)

Divalent and Mixed Divalent/Monovalent Conduction in β''-Alumina: A Monte Carlo Study

ALEXANDER PECHENIK AND D. H. WHITMORE

Department of Materials Science and Engineering and Materials Research Center, Northwestern University, Evanston, Illinois 60201

AND MARK A. RATNER

Department of Chemistry and Materials Research Center, Northwestern University, Evanston, Illinois 60201

Received September 4, 1984; in revised form October 29, 1984

A Monte Carlo method is developed for simulation of mixed ionic conductivity in β''-alumina-type materials. The conduction plane of these materials is represented by a lattice gas model in which monovalent and divalent cation carriers diffuse via a vacancy mechanism and interact through a nearest-neighbor coulombic repulsion. By comparing experimental data for pure Na^+ and pure Ba^{2+} β''-aluminas with simulation results, it is possible to estimate the near-neighbor interaction energies ε_i and jump barriers U_i for both kinds of ions. On the basis of these estimations the total ionic conductivity of Na^+–Ba^{2+} β''-alumina is calculated as a function of temperature and concentration of carriers. As Ba^{2+} replaces Na^+, the conductivity initially increases as more vacancies become available. For very high temperatures, this increase continues until exchange is complete; but at lower temperatures, the conductivity reaches a peak for some optimal Ba^{2+}/Na^+ composition, and then drops off as the number of Ba^{2+}, and hence the strength of ionic correlation, goes up. The presence of ordering in the fully exchanged (all Ba^{2+}) case manifests itself in substantial curvature of the Arrhenius plots for conductivity. The activation energy for conductivity as a function of Ba^{2+} mole fraction ($X_{Ba^{2+}}$) shows a pronounced rise near an X value of $\frac{2}{3}$, in agreement with recent experimental observations.

I. Introduction

The β-alumina family represents one of the most important classes of framework solid electrolytes. Since their discovery in the 1960s, these materials have come under intense scrutiny both for intrinsic scientific reasons (fast-ion conductors with ionic motion largely restricted to two dimensions) and for electrochemical cell applications. Various singly charged cations, including Ag^+, Na^+, Li^+, K^+, and H^+, have been shown to be quite mobile in either β-alumina or β''-alumina or both (useful reviews are found in Ref. (*1*)). Recent work in several laboratories (*2–5*) has demonstrated that certain doubly charged cations (Ca^{2+}, Sr^{2+}, Pb^{2+}, Ba^{2+}) may be introduced into the conduction slabs of the β''-aluminas by ion exchange. These exchanged materials also exhibit fast-ion conduction, albeit usually lower than the monovalent cations. The Pb^{2+}, in particular, shows anomalously high conductivity (*4, 5*).

0022-4596/85 $3.00

Several interesting mechanistic questions arise in attempting to understand the conductivity of β''-aluminas with mobile divalent cations (M^{2+}). The increased charge should lead both to stronger lattice polarization effects and to stronger coulombic interactions, while the preparative method (ion exchange) assures that the M^{2+} salt will have more available vacant sites for ions to occupy. In addition, the theoretical suggestion (*6, 7*) that a local minimum in conductivity should occur for commensurate stoichiometries (in which the number of ions is the site number divided by an integer), which has been made for one-dimensional models, might imply, if extended to two-dimensional materials of the β-alumina type, that local conduction minima and ion ordering should occur for commensurate geometries such as a 50% full lattice (this same result, for β''-alumina, follows from Monte Carlo (*8*) and path-probability calculations, see Ref. (*9*)). To understand the magnitude and mechanisms of transport in these substances, we have carried out Monte Carlo (MC) calculations using a method similar to that of Murch and Thorn (*8, 10, 11*). We report here our results for the Na^+/Ba^{2+} β''-alumina system. This system has been chosen because both Na^+ and Ba^{2+} ions mostly reside on Beevers–Ross sites (*12*); thus, mid-oxygen sites, which play an important role in the conduction process for β''-aluminas containing the mobile species Sr^{2+}, Ca^{2+}, Zn^{2+}, and Cd^{2+}, can be excluded from our model.

Experimental work by Dunn and Farrington (*5*) has shown that the Ba^{2+} material is a moderately good conductor, and has determined its activation energy for conduction. Our calculations, which are based on a lattice gas hopping model with nearest-neighbor repulsion, show that correlation effects among ions, which can lead to ordering and consequently lowered conductivity even for monovalent cations if the per-site ion density ρ is close to the commensurate value of 0.5, are considerably enhanced for Ba^{2+}, thereby leading to strong ordering effects even at relatively high temperatures and to curvature in the Arrhenius plot. As Ba^{2+} replaces Na^+ in the lattice, the conductivity initially rises. At high temperatures, this behavior continues until full exchange is obtained; but, for lower temperatures in the usual experimental range, the total conductivity reaches a maximum for some intermediate exchange, then diminishes due to strong correlations when even more Ba^{2+} replaces the Na^+ ions.

Section II describes our lattice gas hopping model and outlines the procedure used for evaluation of the parameters for MC simulation, which are the activation energies, U_{Na} and U_{Ba}, and near-neighbor repulsion energies ε_{Na} and ε_{Ba}; these are chosen by fitting to the reported conductivity data for pure Na^+- and Ba^{2+}-β''-aluminas. Section III outlines the Monte Carlo procedure used. Section IV discusses the partially exchanged materials, including the conductivity expected for the equilibrium crystals as a function of Ba^{2+} concentration and temperature.

II. The Model and Parameter Evaluation

We have assumed a honeycomb lattice, with all lattice sites equivalent. The lattice geometry is assumed independent of mobile-ion concentration or charge. The mobile-ion behavior is then modeled as that of a lattice gas with interactions permitted only between nearest neighbors. For the pure Na^+ case, conduction occurs by a vacancy mechanism (for one set of experiments (*3*), the mobile-ion lattice is 92.7% full for this situation). There are three interaction energies for nearest-neighbor barium and sodium ions, denoted by ε (for Na^+–Na^+), by 2ε (for Na^+–Ba^{2+}), and by 4ε (for Ba^{2+}–Ba^{2+}). The value of ε, which corre-

sponds roughly to a strongly screened Coulomb potential, will be determined below.

Assuming that migration of both sodium and barium ions follows the vacancy mechanism, the total conductivity for the system, σ_t, can be written as the sum of the partial conductivities σ_{Ba} and σ_{Na}:

$$\sigma_t = C_{Ba}q_{Ba}\mu_{Ba} + C_{Na}q_{Na}\mu_{Na} \quad (1)$$

for the case in which both ions are present in the conduction slab. Here μ_i's are the mobilities of the respective ions, C_i's the concentration of carrier i, and the q_i's the electric charge associated with a given ion.

The generalized Nernst–Einstein relation (*11*) may be used for determination of μ_i

$$\mu_i = D_{c_i}\frac{q_i}{kT}, \quad (2)$$

where D_{c_i} is the charge diffusion coefficient, which can be calculated using the Monte Carlo (MC) method developed by Murch and Thorn (*8, 10*). One then writes for the charge diffusion coefficient:

$$D_{c_i} = \frac{\lambda^2\Gamma_i}{3}f_{c_i}, \quad (3)$$

where the 3 is a geometric factor appropriate to the honeycomb lattice, λ is the length of a unit jump, f_{c_i} is the charge correlation factor, and Γ_i is the jump frequency. The Γ_i can be written as (*9, 10*)

$$\Gamma_i = 3\nu_i V_i W_i e^{-U_i/kT}, \quad (4)$$

where U_i is the activation energy for the ith ion in an empty lattice, ν_i is the vibrational contribution to the jump frequency, V_i is the so-called vacancy availability factor, and W_i is the effective jump frequency factor. The factors V_i and W_i, originally introduced by Sato and Kikuchi (*9*), refer to configurational properties of the lattice gas and can be straightforwardly calculated from the MC simulation.

A method for calculation of f_{c_i} has been given by Murch (*8, 10, 11*) and consists of first applying a permanent electrostatic field to the crystal and subsequently calculating the average drift distance of the ions:

$$f_{c_i} = \frac{2kT\langle x\rangle}{q_iEnx^2}, \quad (5)$$

where E is the applied field, n is the number of jumps per ion, and x is a projection of the jump distance λ on the field direction x. Finally, if V_i, W_i, f_{c_i} are calculated, the conductivity, using Eqs. (1), (2), and (3), is simply given by

$$\sigma_t \propto C_{Ba}\cdot q_{Ba}^2\cdot D_{c_{Ba}} + C_{Na}\cdot q_{Na}^2\cdot D_{c_{Na}} \quad (6)$$
$$\propto C_{Ba}\cdot 4\cdot D_{c_{Ba}} + C_{Na}\cdot D_{c_{Na}}.$$

There are two parameters in Eq. (4) that remain to be determined, namely the vibrational contribution to the jump frequency, ν_i, and the activation energy for a unit jump with no occupied neighbor sites, U_i. Since σ_t in Eq. (6) is measured in arbitrary units it is only the ratio of ν_{Na}/ν_{Ba} that is significant in this calculation. We assume, here, that

$$\frac{\nu_{Na}}{\nu_{Ba}} = \sqrt{\frac{m_{Ba}}{m_{Na}}}, \quad (7)$$

which corresponds to a harmonic approximation for the vibration of the sodium and the barium ions, and is consistent with the static lattice assuming ν_i is independent of temperature and stoichiometry of the material. The activation parameter U_i and the repulsive strength ε may be calculated by comparison with the pure materials. Ni *et al.* (*3*) give the activation energy for pure Na^+ β''-alumina single crystal as 0.13 eV, when the sites are 92.7% occupied by Na^+. Dunn and Farrington (*2*) give the activation energy for pure Ba^{2+} β''-alumina as 0.58 eV, with the fraction of occupied sites equal to one-half of that for Na^+ ions; for their material in pure Na form, the percentage of occupied sites (86%) is slightly lower than in the material of Ref. (*3*). We start our parameter-fitting procedure with the general

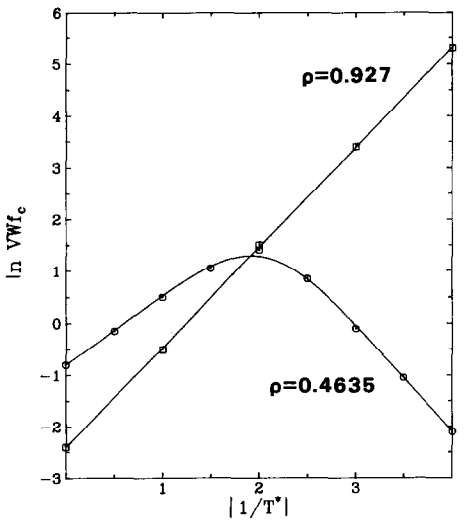

FIG. 1. Calculated temperature dependence of the VWf_c product for β''-alumina. The pure Na and pure Ba limits lie at $\rho = 0.927$ and $\rho = 0.4635$, respectively.

equation for ionic conductivity given by Sato and Kikuchi (*9*),

$$\sigma T = K \cdot V \cdot W \cdot f_c \cdot e^{-U/kT}, \qquad (8)$$

where K is a temperature-independent constant. Then we obtain

$$\frac{\partial \ln(\sigma T)}{\partial(1/T)} = \frac{\partial \ln(VWf_c)}{\partial(1/T)} - \frac{U}{k}. \qquad (9)$$

The left-hand side of Eq. (9) is equal to the observed value of activation energy ($E_a \equiv \partial \ln(\sigma T)/\partial(1/T) = 0.13$ eV for Na^+ and 0.58 eV for Ba^{2+}). On the right-hand side of Eq. (9), we have a sum of the terms: $-U/k$ which represents the "pure" activation energy for a particle jumping out of a potential well, and $\partial \ln(VWf_c)/\partial(1/T)$ which results from interactions between particles.

The dependence of $\ln VWf_c$ on T^* ($\equiv kT/\varepsilon$) has been reported (*14*) and, for the two cases under investigation, the curves of Fig. 1 are obtained. Note that, following Sato and Kikuchi (*9*), ε is defined as a pairwise interaction energy between two ions on neighboring lattice sites. In their convention, $\varepsilon > 0$ represents an attractive energy, whereas $\varepsilon < 0$ represents a repulsive energy. Thus, a tendency for ordering of the ions and vacancies on the honeycomb lattice of the β'' structure at lower temperatures ($\varepsilon < 0$) is represented here by a negative T^* value. While this definition seems contrary to the usual coulombic sign convention, it is standard in the ionic conductor literature, and we retain it here: both ε and T^* are negative, by this convention of Sato and Kikuchi, for repulsive ion–ion interaction.

We have assumed that $\varepsilon_{Ba} = 4\varepsilon_{Na}$; thus, $T^*_{Ba} = \frac{1}{4}T^*_{Na}$ for any temperature T. Since the experimental data for Ba^{2+} β''-alumina show completely Arrhenius behavior (*5*), the low-temperature parts of the curves in Fig. 1 have to be used. Then for pure Ba^{2+} we observe, from these curves, that

$$\frac{\partial \ln(\sigma T)}{\partial(1/T)} = -\frac{U_{Ba}}{k} - \frac{1.5|\varepsilon_{Ba}|}{k} = -\frac{U_{Ba} + 6|\varepsilon_{Na}|}{k} = \frac{0.58 \text{ eV}}{k} \qquad (10)$$

and for pure Na

$$\frac{\partial \ln(\sigma T)}{\partial(1/T)} = -\frac{U_{Na}}{k} + \frac{2|\varepsilon_{Na}|}{k} = -\frac{U_{Na} - 2|\varepsilon_{Na}|}{k} = \frac{0.13 \text{ eV}}{k}. \qquad (11)$$

(The values $-1.5|\varepsilon|$ and $+2|\varepsilon|$ are read from the slopes of the curves of Fig. 1). Thus, we find that

$$U_{Ba} + |6\varepsilon| = 0.58 \text{ eV} \qquad (12)$$

$$U_{Na} - |2\varepsilon| = 0.13 \text{ eV}. \qquad (13)$$

Finally, using Eq. (8):

$$\frac{\sigma_{Na}}{\sigma_{Ba}} = \frac{K_{Na}}{K_{Ba}} \cdot \frac{V_{Na}W_{Na}f_{cNa}}{V_{Ba}W_{Ba}f_{cBa}} \cdot \frac{e^{-U_{Na}/kT}}{e^{-U_{Ba}/kT}}. \qquad (14)$$

The ratio K_{Na}/K_{Ba} depends on geometry of the lattice and the vibrational contributions to the jump frequency, ν_i, as well as occupation numbers, ρ_i, for both systems. From Eqs. (3), (4), (6), (7), and (8) we find that

$$\frac{K_{Na}}{K_{Ba}} = \frac{C_{Na}}{C_{Ba}} \cdot \frac{q_{Na}^2}{q_{Ba}^2} \cdot \frac{\nu_{Na}}{\nu_{Ba}}$$

$$= \frac{0.927}{0.4635} \cdot \frac{1}{4} \cdot \sqrt{\frac{137}{23}} = 1.22. \quad (15)$$

The ratio σ_{Na}/σ_{Ba} at any fixed temperature is known from the experimental data (*2, 3*); thus Eqs. (12), (14), and (15) can be solved to give ε. We have adopted the following procedure to obtain ε:

(1) For $T = 300°C$, the ratio σ_{Na}/σ_{Ba} was taken from experiment (*2, 3*).

(2) The chosen temperature was arbitrarily assigned to correspond to some T^* value, thus fixing ε.

(3) Equations (12), (13), and (14) were solved to give ε.

(4) If the calculated value of ε was different from the experimental one, as determined from the slope of Fig. 1, then another value for T^* was chosen and the whole procedure repeated.

This procedure yielded the following results:

$$\varepsilon_{Na} = -0.04 \text{ eV} \quad (16)$$

$$U_{Na} = 0.21 \text{ eV} \quad (17)$$

$$U_{Ba} = 0.34 \text{ eV}$$

$T = 300°C$ corresponds to $T^* = -1.2$.

These parameters were then used in MC calculations of the conductivity.

III. The Monte Carlo Procedure

The MC technique of Murch and Thorn (*8*) was adopted with minor modifications. Sodium, barium ions, and vacancies were initially introduced at random into an array of 3200 sites on a honeycomb lattice. The number of charge carriers of a certain type was determined using the charge neutrality requirement and keeping in mind that every Ba^{2+} ion substitutes for two Na^+ ions; thus the number of vacancies increases significantly when Ba^{2+} is exchanged for Na^+. Thus

$$\rho_{Ba} = \frac{\rho_0 X}{1 + X}$$

$$\rho_{Na} = \rho_0 \frac{1 - X}{1 + X}, \quad (18)$$

where $\rho_0 = 0.927$ is the initial occupational number for the pure sodium crystal and

$$X = \frac{\rho_{Ba}}{\rho_{Ba} + \rho_{Na}} = \frac{C_{Ba}}{C_{Ba} + C_{Na}}. \quad (19)$$

The MC calculations were carried out using the importance-sampling method of Metropolis *et al.* (*15*) (whose application to lattice hopping problems has been discussed in several references (*10, 13*)) to prepare the equilibrium ensemble. The actual conductivity calculations employed the technique of Murch (*8, 10*), and have been discussed elsewhere (for application to correlated motion mechanisms in Na-β''-alumina, cf. Ref. (*13*)). From these numerical data, the following parameters have been calculated:

(a) The vacancy availability factors, V_{Na} and V_{Ba}, are obtained as average numbers of vacancies encountered in the simulated motion of Na^+ and Ba^{2+} ions, respectively;

(b) the effective jump frequency factors W_{Na} and W_{Ba}, found from the equation

$$W_i = P_i/V_i e^{-U_i/kT}, \quad (20)$$

where P_i is the average jump probability for one kind of charge carrier; and (c) the charge correlation factor for each ion type, obtained from Eq. (5).

IV. Results

The MC simulations give not only the total ionic conductivity, σ_t, and the partial conductivities, σ_{Ba} and σ_{Na}, but also the factors V, W, and f_c for each ion type, which permits interpretation of the changing and competing roles of vacancy avail-

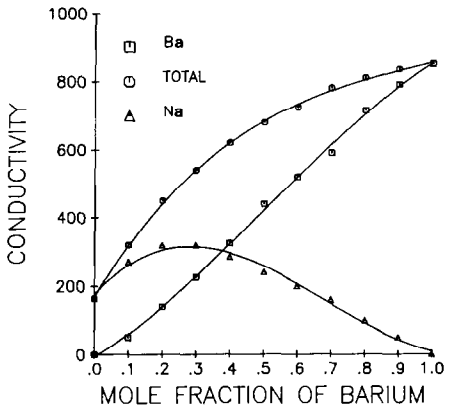

FIG. 2. The calculated ionic conductivity of the mixed Na/Ba system, for $T^* = kT/\varepsilon = \infty$, corresponding to very high temperature.

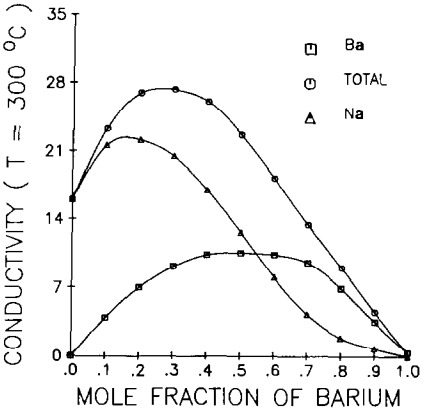

FIG. 4. As in Fig. 3, for $T = 300°C$. Note pronounced maximum in total conductivity.

ability and ionic correlation. The results of the MC simulation are presented in Figs. 2–14. The total conductivity of the material and partial conductivities for Na and Ba as functions of the Ba^{2+} mole fraction X, defined in Eq. (19), are shown in Figs. 2–5. Thus $X = 0$ represents the pure sodium case, with the concentration of sodium ions on the conduction plane equal to 0.927, $X = 1$ corresponds to the pure Ba case with $\rho_{Ba} = 0.927/2 = 0.4635$. As X goes from 0 to 1, one Ba^{2+} replaces two Na^+ in the body of the crystal. Figure 2 shows the conductivity when no interactions exist between the charge carriers except for blocking of the sites on the conduction plane ($\varepsilon \to 0$, or $T^* \to -\infty$); this case can be regarded as a high-temperature limit. Here σ_t rises steadily due to the contribution arising from the mobile Ba^{2+} ions. The sodium conductivity initially rises, due to the increase of a number of vacancies in the conduction plane, and maximizes at $X_{Ba} \cong 0.2$, after which σ_{Na} gradually goes to zero as sodiums disappear from the system. It is helpful to analyze the situation in terms of V_i, W_i, and f_{ci} which are defined in Section II. According to Eq. (8):

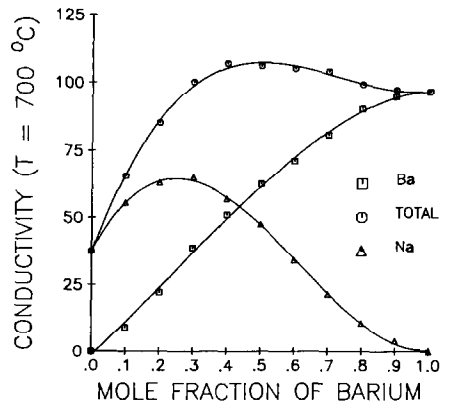

FIG. 3. As in Fig. 2, for $T = 700°C$.

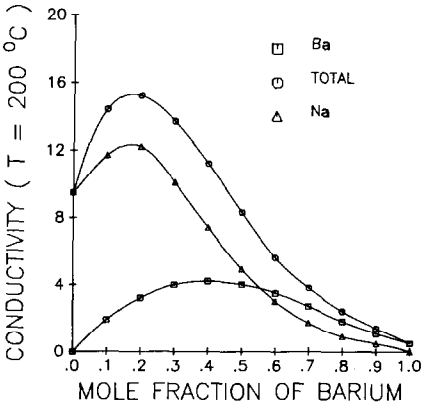

FIG. 5. As in Fig. 4, for $T = 200°C$.

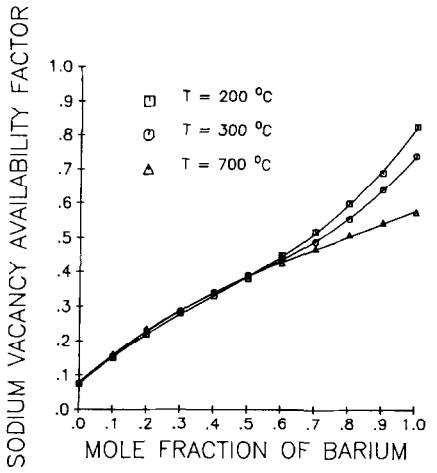

FIG. 6. Calculated dependence of V_{Na} factor on mole fraction.

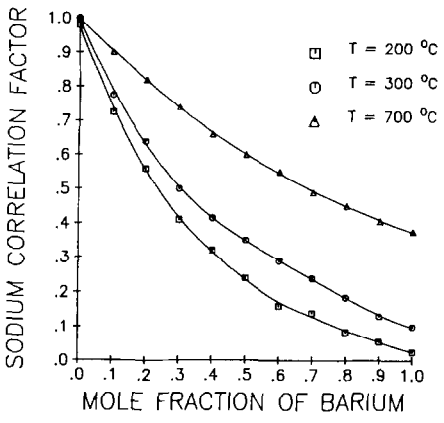

FIG. 8. Calculated dependence of f_{Na} factor on mole fraction.

$$\sigma_i T = K_i V_i W_i f_{c_i} e^{-U_i/kT}, \quad \text{(where } i = \text{Na,Ba)}$$

and since $K_i \propto \rho_i$

$$\sigma_i T \propto \rho_i V_i W_i f_{c_i}. \tag{21}$$

Thus, we can understand the temperature and composition dependence of conductivity by comparing Figs. 2–5 with Figs. 6–11, which give important information about the details of the conduction process.

The conductivity is essentially [Eq. (21)] given by the product VWf_c. The local peak in σ_t as a function of X, seen in Figs. 3–5, must then be due to structure in these three factors. The vacancy availability V (Figs. 6, 9) increases monotonically with X, since each Ba^{2+} brings with it an additional vacancy. The vacancy availability factor, V, decreases very slightly with increasing T, since at low T, the repulsive interaction ε will cause each ion to surround itself with vacancies to whatever extent it can; as the

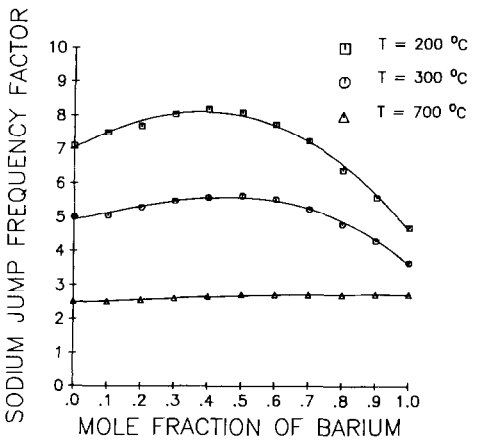

FIG. 7. Calculated dependence of W_{Na} factor on mole fraction.

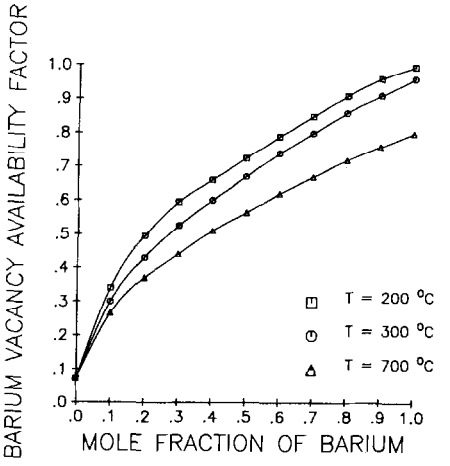

FIG. 9. Calculated dependence of V_{Ba} factor on mole fraction.

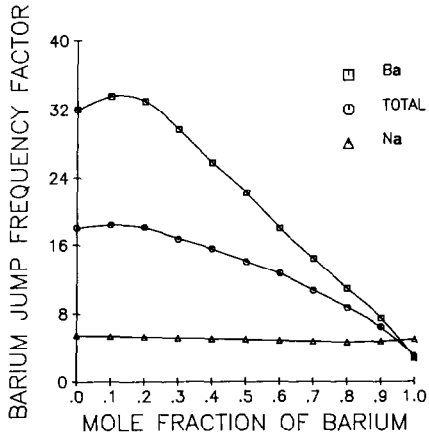

FIG. 10. Calculated dependence of W_{Ba} factor on mole fraction.

temperature increases, this ordering will diminish, as will the value of V. The W factor measures the influence of neighboring ions on the jump frequency of the carriers and for high temperatures, W is essentially independent of X (Figs. 7, 10). Thus, the curvature and maximum observed for σ_t at 700°C, is not due to V or W, but must arise from the correlation factor f_c. Figures 8 and 11, indeed, show that, as $[Ba^{2+}]$ increases and the ionic repulsions increase in strength, f_c drops significantly. Accordingly, the peak in σ_t can be qualitatively understood as being due to an initial rise in the vacancy availability factor, V, which is eventually reversed by a strong charge correlation effect.

Another way of looking at this process is to consider the phase diagram for the honeycomb lattice (*14*). The pure Ba^{2+} case ($\rho = 0.4635$, $X = 1$) lies within the long-range ordering region of this system with the critical temperature, $T^* \cong -0.4$ (From Eq. (16), this is roughly 490°C). Figure 3 shows that, for Na, $T^* = kT/\varepsilon_{Na} = -2.0$, and for Ba, $T^* = kT/\varepsilon_{Ba} = -0.5$. Thus, when $X \rightarrow 1$, Ba^{2+} ions try to order themselves on the lattice, leading to highly correlated motion for *both* Ba^{2+} and Na^+ ions. (Although long-range order has not been established at $T^* = -0.5$, the correlation length has already increased dramatically (*14*).)

The transition from long-range order (which occurs for $0.41 \leq \rho \leq 0.59$ at sufficiently small $|T^*|$) to short-range order occurs as T is increased. It results in curvature of the activation plot, but not in abrupt change either in slope or in value. Such second-order transitions should exhibit sharp changes in second-derivative thermodynamic properties such as heat capacity, and vanishing of order parameters, as the transition occurs, but transport properties, such as σ, do not necessarily change abruptly.

Figures 4 and 5 represent 300 and 200°C, respectively ($T^* = -1.2$ and -1.0). For the pure Ba case $T^*_{Na} = -1.2$ corresponds to $T^*_{Ba} = -0.3$; thus, both temperatures are below the critical temperature.

The effects of ordering are clearly shown in Figs. 4 and 5. As X increases, Ba ions surround themselves with vacancies, leading to the formation of a long-range ordered superlattice. Both Na and Ba ions execute correlated motion through the lattice with correlation factors close to zero. The factors V_{Na} and V_{Ba} go even higher, since at low temperatures both ions try to surround

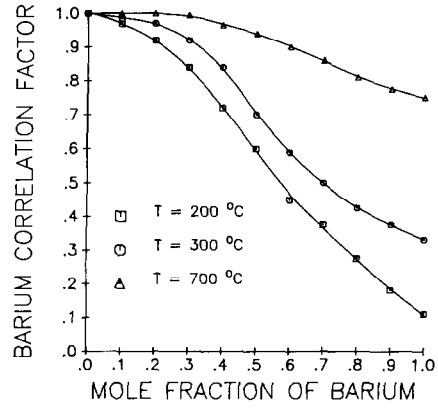

FIG. 11. Calculated dependence of f_{Ba} factor on mole fraction.

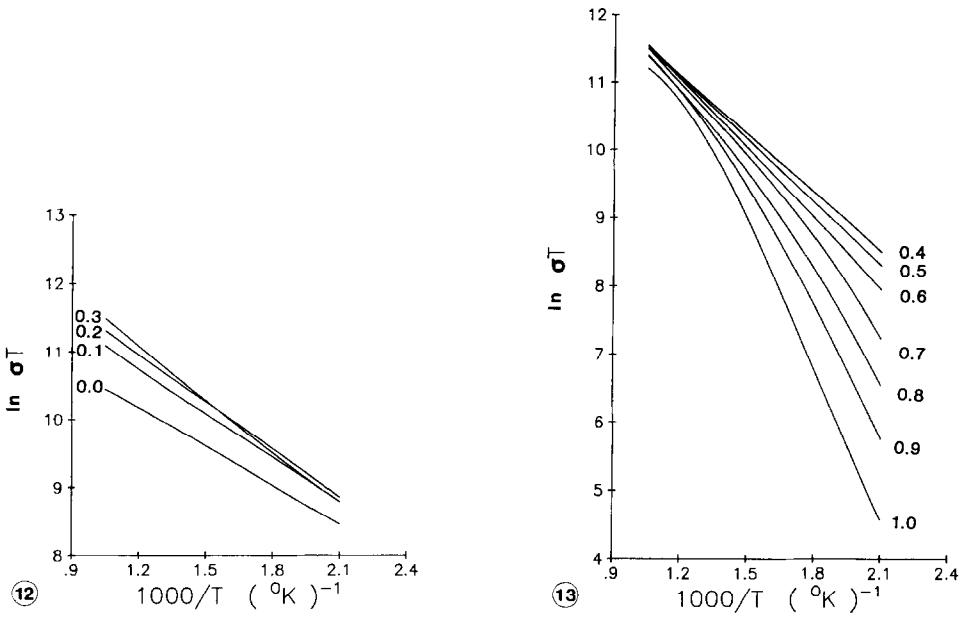

FIGS. 12, 13. Activation plots for total conductivity. Lines represent the mole fraction of Ba. Note pronounced curvature, due to strong correlation effects, for pure Ba case (compare with Fig. 1).

themselves with vacancies. This effect causes a slight initial increase in ionic conductivity at a small X, but the strong interactions between Ba–Ba and Ba–Na neighboring ions soon lead to a decrease in conductivity for larger X.

In Fig. 8, one can see that the sodium charge correlation factor for the case of noninteracting particles is less than unity. This cannot be fully explained without a lengthy discussion (*10, 16*) about the physical meaning of the charge correlation factor, f_{c_i}, but we note that it is the difference in mass between sodium and barium ions, and consequently the difference in the jump escape frequencies, which causes this correlation effect even when there is no interaction between ions (except site blocking).

Figures 12 and 13 show Arrhenius plots calculated from the MC simulation for different values of X. Two features of these plots are noteworthy: (i) for $X \rightarrow 0$, the system displays perfect Arrhenius behavior with activation energy, E, increasing with increase of X; and (ii) for $X > 0.7$ the plots exhibit non-Arrhenius behavior, the curvature becoming greater as $X \rightarrow 1$ and correlation effects predominating.

This departure from the Arrhenius-type behavior is caused by the order–disorder transition which Ba ions undergo as $X \rightarrow 1$

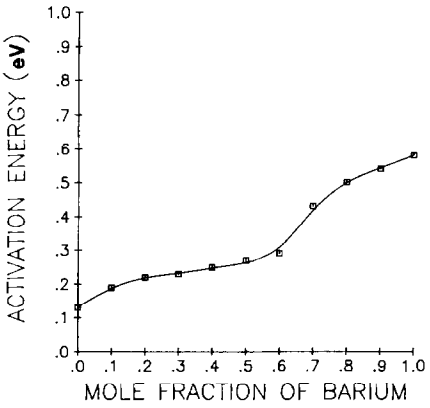

FIG. 14. Calculated activation energy (from Figs. 12 and 13). For large Ba concentrations, the low-temperature value of E_a is used.

for $T < 490°C$. The onset of the long-range order drastically decreases the conductivity in the system and causes the ln σT vs $1/T$ plot to bend downward at low temperatures. Just such behavior has in fact been reported for Eu^{3+} β''-alumina (*17*).

Finally, Fig. 14 shows the variation of E_a with X. As X goes up, the activation energy goes up, as one would expect. For the curved plots (large Ba concentrations) we used the low-temperature results for calculation of the activation energy.

V. Remarks

While the Na^+ β''-aluminas have been known for quite some time, the recent preparation (*2–5, 17*), by ion exchange, of materials containing divalent cations (Ba^{2+}, Ca^{2+}, Pb^{2+}) and trivalent cations (Eu^{3+}) ions in the conduction slab permits continuous tuning of the ion density and the strength of coulombic correlation among the hopping ions. In the case of very strong coulombic interactions, the site hopping model becomes invalid as the ions should move in a liquid-like fashion (*18*); still one suspects that, for the Ba^{2+} case, the hopping model is valid. Indeed, in the diffraction data of Thomas *et al.* (*12*), the ions are largely localized about Beevers–Ross and mid-oxygen positions. Thus, the lattice gas hopping model which we have employed here seems justified (the liquid-like behavior will start to occur for $|\varepsilon| \cong U$, and from Eqs. (16) and (17) it is seen that $|\varepsilon|$ is still well below this range).

Our calculations make an interesting experimental prediction: notably, a local maximum in the conductivity should be evident for partial Na^+/Ba^{2+} exchange (Figs. 3–5). While some experimental papers have considered conduction in mixed monovalent–divalent β-aluminas, we know of none which have precisely the conditions employed in our model calculations. Farrington's group (*19*) has studied the problem in the β (not β'') structure, and observes a change in mechanism (from interstitialcy to vacancy) as the divalent cation concentration increases. They also found an increased conductivity upon initial exchange. Ni *et al.* (*3*) did study partially exchanged Na^+/Ca^{2+} β''-alumina, and observed a rapid fall-off in σ_t for small $\rho_{Ca^{2+}}$. However, their measurements were made on a nonequilibrium crystal, in which the ionic exchange process resulted in a sharp gradient in calcium concentration from the surfaces of the crystal to its interior ("picture frame" effect). The initial sharp decrease in σ_t observed for the case where only a small amount of calcium has been exchanged into the sample arises from replacement of a mobile Na^+ by the less-mobile Ca^{2+} near the electrode/electrolyte interface, as the Ca^{2+} strongly bind the vacancies, thus reducing V for Na^+ motion to the interface. Such "picture frames" have been noted earlier (*20*). Work is now under way in our laboratory on a true equilibrium study of σ_t for a partially exchanged monovalent/divalent cation–β''-alumina system.

Acknowledgments

We are grateful to G. C. Farrington and B. Dunn for helpful comments, and to the AFOSR, DOE, and the NSF-MRL program for support of this research (through Grants AFOSR-82-0221B, DMR82-16972, and DE-AC02-76ER02564).

References

1. G. C. Farrington and J. B. Bates, Eds., "Fast Ionic Transport in Solids," North-Holland, Amsterdam (1981); P. Vashishta, J. N. Mundy, and G. K. Shenoy, Eds., "Fast-Ion Transport in Solids," North-Holland, Amsterdam (1979).
2. B. Dunn and G. C. Farrington, *Mater. Res. Bull.* **15,** 1773 (1980).
3. J. Ni, Y. T. Tsai and D. H. Whitmore, *Solid State Ionics* **5,** 199 (1981).
4. B. Dunn, R. Ostrum, R. Seevers, and G. C. Farrington, *Solid State Ionics* **5,** 203 (1981).
5. G. C. Farrington and B. Dunn, *Solid State Ionics* **7,** 267 (1982).

6. T. GEISEL, *Phys. Rev.* B20 (1979) 4294.
7. S. H. JACOBSON, A. NITZAN, AND M. A. RATNER, *Phys. Rev.* B23 (1981) 1580; M. A. RATNER, *Acc. Chem. Res.* **15,** 355 (1982).
8. G. E. MURCH AND R. J. THORN, *Philos. Mag.* **36,** 529 (1977); **35,** 493 (1977).
9. H. SATO AND R. KIKUCHI, *J. Chem. Phys.* **55,** 677, 702 (1971).
10. G. E. MURCH, "Atomic Diffusion Theory in Highly Defective Solids," TransTech, Aedermansdorf (1980).
11. G. E. MURCH, *Solid State Ionics* **7,** 177 (1982).
12. J. O. THOMAS, M. ALDEN, AND G. C. FARRINGTON, *Solid State Ionics* **9,** 301 (1983).
13. A. PECHENIK, D. H. WHITMORE, AND M. A. RATNER, *Solid State Ionics* **9** and **10,** 287 (1983).
14. A. PECHENIK, D. H. WHITMORE, AND M. A. RATNER, *J. Chem. Phys.,* submitted for publication.
15. N. METROPOLIS, A. W. ROSENBLUTH, M. N. ROSENBLUTH, A. H. TELLER, AND E. TELLER, *J. Chem. Phys.* **21,** 1087 (1953).
16. A. PECHENIK, D. H. WHITMORE, AND M. A. RATNER, to be published.
17. B. GHOSAL, E. A. MANGLA, M. R. TOPP, B. DUNN, AND G. C. FARRINGTON, *Solid State Ionics* **9,** 273 (1983).
18. S. H. JACOBSON, M. A. RATNER, AND A. NITZAN, *Solid State Ionics* **5,** 125 (1981).
19. P. H. SUTTER, L. CRATLY, M. SALTZBERG, AND G. C. FARRINGTON, *Solid State Ionics* **9,** 295 (1983).
20. R. ROMIEU AND A. D. PELTON, *J. Electrochem. Soc.* **128,** 50 (1981).